IEEE Access
Multidisciplinary | Rapid Review | Open Access Journal

Received October 11, 2020, accepted October 18, 2020, date of publication October 27, 2020, date of current version November 10, 2020.

Digital Object Identifier 10.1109/ACCESS.2020.3034122

Dynamic Loading System of an Agricultural Vehicle Power Wagon Based on Complex Loading

XIANGHAI YAN, QIANWEN TAO, AND LIYOU XU

College of Vehicle and Traffic Engineering, Henan University of Science and Technology, Luoyang 471003, China

Corresponding author: Liyou Xu (xlyou2002@sina.com)

This work was supported in part by the National Key Research and Development Program of China during the 13th Five-Year Plan Period under Grant 2016YFD0701002 and Grant 2017YFD070020-402, in part by the Henan University of Science and Technology Innovation Talents Support Program under Grant 18HASTIT026, and in part by the Henan Province Production and Research Cooperation Project under Grant 182107000010.

ABSTRACT A dynamic loading system of a power wagon is studied to solve the problems of low loading precision, slow response speed, and poor adaptive capability of a power wagon in an agricultural vehicle traction test. The load feature of an engine is analyzed under different gear locations, governor handle positions, and vehicle speeds. Meanwhile, the load feature of an eddy current retarder is examined based on a backpropagation (BP) neural network proportional–integral–derivative (PID) control algorithm. The mathematical model for the loading system is established. The time domain model for traction is refactored by a white noise filter according to the power spectral density function. To improve the dynamic loading performance of the eddy current retarder, the BP neural network PID control algorithm is used to change its exciting voltage to achieve an accurate simulation of the actual working load. The effectiveness and practicability of this control algorithm are validated by comparing its system output response dynamic characteristics with those of the traditional PID control algorithm. Simulation results show that the output error is less than 2.8% and the maximum delay is 56.5 ms when the BP neural network PID control is used. On the basis of this result, the traction property of a tractor with several wheels is tested on the road. The test and analysis results indicate that the output loads of the loading system accurately simulate the field actual load of the tractor. The maximum output load value of the system is 42–48 kN and the applicable speed range is 0–25 km/h. The output error is less than 3.5% and the maximum delay is 85.6 ms.

INDEX TERMS Agricultural vehicle, complex loading, dynamic loading, power wagon.

I. INTRODUCTION

A power wagon is an important equipment in vehicle road experiments; it is used to measure the power parameter of a vehicle. The output load of a power wagon loading system can simulate loads under different working conditions in the field [1], [2].

A. APPLICATION OF RETARDER ON VEHICLES

An engine load is the typical loading method for a power wagon. Engine resistance moment is usually verified via bench testing. However, the characteristics of engine resistance moment are rarely studied in the real working environment of a tractor. An eddy current retarder is another loading equipment of a power wagon. The performance of retarder has been studied by local and foreign scholars. Zhang *et al.* [3] proposed a self-excited liquid-cooled eddy current retarder (SL-ECR) structure. The braking performance and power generation performance of the retarder were tested by means of experiments. Xu *et al.* [4] established a 7-DOF vehicle simulation model to analyze the influence of Retarder on braking stability of semitrailer train. Zhao *et al.* [5] studied the actual braking capacity of the combined braking system of permanent magnet eddy current retarder and exhaust brake on automobile, and verified the combined braking performance through tests. Xu and Yu [6] put forward a method to apply eddy current retarder to articulated vehicle by using combined braking system, and its

The associate editor coordinating the review of this manuscript and approving it for publication was Shihong Ding.

braking performance was verified through simulation. Anwar [7] established a parametric model of eddy current retarder based on experimental data, and verified the accuracy of the model through real vehicle test. He *et al.* [8] derived the calculation formula of current density and resistance moment of eddy current retarder by using electromagnetic field theory, which reflected the relationship between design parameters of eddy current retarder. At present, retarders are mainly used in the braking system of vehicles, and the braking performance of vehicles is improved through different control methods. The retarder mainly outputs static torque. However, there are relatively few studies on the use of retarder output torque to dynamically simulate tractor load, and methods have not yet been established.

B. APPLICATION OF OPTIMIZED PID ALGORITHM IN VEHICLE CONTROL

PID (Proportional Integral Derivative) control is a classic control algorithm. Because of its simple algorithm, good robustness and high reliability, it is widely used in industrial process control. Qu *et al.* [9] established a mathematical model of adaptive self-learning and self-organizing PID controller for greenhouse temperature based on RBF neural network. RBF neural network was used to identify the Jacobian matrix of the feedback system, and the PID controller parameters were adjusted online. Chen *et al.* [10] designed a neural network PID adaptive height adjustment controller. The stability and control accuracy of the controller are verified by experiments, which can effectively alleviate vehicle vibration. Yang *et al.* [11] designed a steering controller composed of neural network PID controller and pump motor displacement controller, which realized the steering control strategy of automatically reducing the average vehicle speed and accurately reaching the steering radius expected by the driver. Wang *et al.* [12] proposed a neural network PID control method for adaptive adjustment of gas mass flow, which effectively alleviated the adverse phenomena such as overcharge, over discharge and oscillation in the process of vehicle height adjustment of electronically controlled air suspension. The optimized PID algorithm has stable and reliable performance and is one of the most widely used algorithms in the vehicle field.

C. APPLICATION OF BP NEURAL NETWORK CONTROL ALGORITHM

BP (Back Propagation) neural network is a widely used neural network optimization algorithm. It has been applied in many fields. Xie *et al.* [13] used BP neural network to optimize the structural size of the engineering plane foundation structure. Yang and Shi [14] studied the information fusion state estimation of multi-sensor systems based on the improved BP neural network. He *et al.* [15] used BP neural network to solve the differential equation of plane problems, establishes the algorithm of difference equation, and realizes the search and optimization of the maximum plane. Ding *et al.* [16] established BP neural network model of the material under different heat treatment temperature conditions. Chen *et al.* [17] took the pixel value and 3D coordinate value of the same corner as the input and output of BP neural network respectively, and improved the crossover mutation probability and annealing criterion of genetic simulated annealing algorithm. Li *et al.* [18] used the input and output data of the neural network model to learn the BP neural network, so that the identified BP neural network can show the transmission characteristics of the model, so that the network can accurately predict the firing trajectory of the neural network model. It can not only accurately fit the neural discharge trajectory of the neurons participating in the network training, but also predict the discharge trajectory and peak time of the neurons not involved in the network training, which has a high accuracy in the training process. Han *et al.* [19] established a comprehensive evaluation model of Soil Nutrients Based on BP neural network. It can be seen that BP neural network is widely used in mechanical engineering and is a reliable optimization algorithm.

At present, the loading methods of most power wagons in China are static. Consequently, the load characteristics of a tractor cannot be fully reflected in practice. The current study evaluates the performance of a power wagon loading system. The system is composed of an engine and a retarder that load simultaneously. In addition, this study analyzes the corresponding relationships among engine resistance moment, gear, governor handle position, and tractor speed. The dynamic loading method of the retarder is the BP neural network PID control. Through combined loading, the output load of the power wagon loading system can simulate the actual field load of the tractor. Finally, a YTO-MF554 tractor is used in the experiment, and the loading capability of the power wagon is validated.

II. STRUCTURE OF THE DYNAMIC LOADING SYSTEM

The power wagon is modified from a YTO-LX1304 tractor. The motive power shaft of the tractor is connected to an eddy current retarder via a universal joint. The power wagon loading system is composed of retarder braking and engine resistance. These two forces establish coupling in the driven bevel gear of the main reducer. The output loading of the power wagon is composed of the two forces and wheel rolling resistance. The structure of the combined loading system is shown in Fig. 1.

The combined loading system is composed of the retarder and engine subsystems. The former includes the power pack, loading controller, sensors, and retarder. The power pack includes the battery, inverter, and DC regulated power. Battery voltage is 24 V, which is converted into 220 V AC by the inverter. DC regulated power can output 0–30 V of direct current. The controller regulates DC regulated power output voltage to control the retarder resistance moment. The sensors include current and force sensors. The current sensor monitors the charge–discharge state of the battery, whereas the force sensor tests the output loading of the power wagon. The test values are feedbacked to the loading controller.

The engine subsystem includes the engine and transmission. The upper computer shows the testing interface, which transports data to the controller. Data acquisition is achieved by the wireless transmission module. The parameters of the devices shown in Fig. 1 are listed in Table 1.

TABLE 1. Main technical parameters of the devices.

Name	Model	Major features
Inverter	JYP-4000W	Output power: 4000 W Inversion efficiency: 90%
DC regulated power		MAX power: 6000 W
Current sensor	LHB-100A	Rated current: 100 A Precision: ±0.5%
Force sensor	BLR-1/10000	Ranges: 10000 kg Overload: 20% R.L.
Retarder	KBG100	MAX current: 56 A MAX torque: 1000 N•m
Wireless module	YL-500IW	Transmitting rate: 9600 bps Transmitting range: ≥3 km

III. ENGINE LOADING SUBSYSTEM

A. ENGINE BRAKING CHARACTERISTICS

The driving wheel that passes a transmission system is the one that drives the engine to turn in reverse. Friction between engine mechanical structures produces resistance. Engine braking power is related to two factors: average friction pressure and total cylinder volume. It is 20%–45% of the rated power.

Engine resistance moment is transmitted to the driving wheel as the engine loading of the power wagon. Different gear locations, throttle lever positions, and vehicle speeds influence engine loading, and thus, determining engine performance via theoretical deduction is difficult. This study investigates the relations between speed and engine loading under different gear locations and governor handle positions.

B. ENGINE LOADING MATCHING

Research on the corresponding relations among the braking load of the engine, the gear, and the position of the governor handle is conducted with the power wagon driving at a steady speed while being pulled by the test vehicle.

The test scheme is as follows.

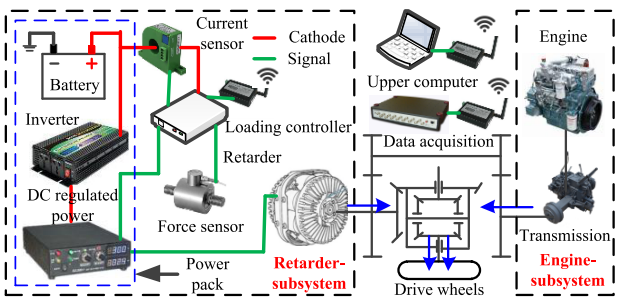

FIGURE 1. Schematic of the loading system.

1) The gear of the power wagon is in neutral, whereas that of the tested vehicle is in low second. The power wagon is driving at a steady speed while being pulled by the test vehicle. Its rolling resistance is measured using a drawing force transducer.

2) The gear of the power wagon is in the middle first under the same road conditions. The position of the governor handle of the power wagon is at 25%. The gear of the tested vehicle is in low second, and the power wagon is driving at a steady speed while being pulled by the test vehicle. Speed is measured using a Global Positioning System speed sensor, whereas traction is measured using a drawing force transducer. The braking load of the engine of the power wagon under different gears, speeds, and positions of the governor handle are measured using the same method. The test data are provided in Fig. 2 when the mobile dynamometer is in the middle second gear and the position of the governor handle is at 50%.

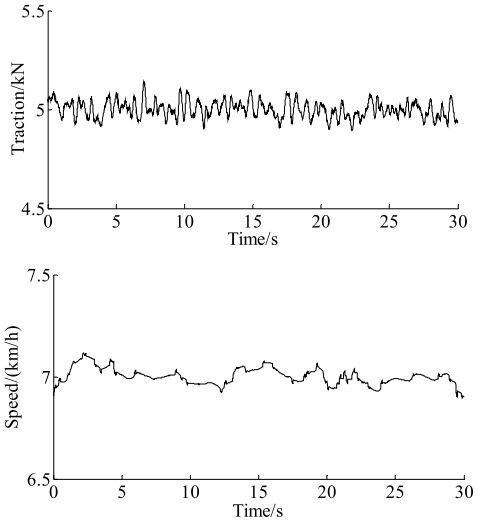

FIGURE 2. Experimental data in M-II-50%.

The rolling resistance of the power wagon measured in the test is 1.52 kN. Several test data can be obtained from Fig. 2. The average traction is 5.06 kN, and the mean speed is 7.12 km/h. The braking load of the engine of the power wagon is 3.54 kN. All the test data are processed, and the corresponding relations among the engine brake load, the gear, and the position of the governor handle can be obtained. The corresponding relations are listed in Table 2.

TABLE 2. Engine loading corresponding relations.

Gear	Governor handle position (%)	Speed (km/h)	Engine loading (kN)
M-I	25	2–4	12–16
M-I	50	3.5–5.5	11.5–15
M-II	25	3.5–6	9.5–11.5
M-II	50	6–8.5	3–5
M-III	25	4.5–7	9.5–9
M-III	50	7.5–10	2–3

Some information can be deduced from Table 2. For example, when the position of the governor handle is larger, engine resistance will be lower under the same gear. When the gear is lower, engine resistance will be lower in the same position of the governor handle. Moreover, with the same gear and position of the governor handle, engine resistance increases as vehicle speed increases.

In the traction performance test, the change in vehicle speed is minimal, such that the braking load of the engine remains stable. The test gear of the test vehicle shows that the gear and the position of the governor handle of the power wagon can be identified from Table 2.

IV. RETARDER LOADING SUBSYSTEM

The tractor field work load is the expected output value in the traction performance test. The engine can only have a stable load; hence, the remaining expected output load is compensated by retarder loading. The output load of the retarder is random, time-varying, and must be adjusted in real time.

A. MODEL FOR RETARDER LOADING

When the retarder is energized, the winding of the retarder generates a magnetic field. The rotor disc is driven by the drive wheels and passes through the transmission system to generate eddy currents. The movement of the rotor disc is hindered in the magnetic field. Therefore, the retarder will generate resistance moment, which can be changed by changing the input voltage.

The resistance moment of the retarder is determined by its structure, material, and rotational speed. Moreover, the dynamic model for the transmission system is affected by the rotary inertia of its components, rigidity, torsional vibration, and other factors. Therefore, establising the model through the mechanism is difficult. The system is single-input and single-output; hence, the experimental method is used to establish the mathematical model for the loading system. Meanwhile, the identification method of step response is used in the test.

The test conditions are as follows: the test pavement is concrete, pavement slope is less than 0.5%, temperature is 22°C, pressure is 100 kPa, and relative humidity is 45%.

The test scheme is as follows.

1) The gear of the mobile dynamometer vehicle is in neutral, whereas that of the test vehicle is in low second. The mobile dynamometer vehicle is driving at a steady speed while being pulled by the test vehicle.

2) The voltage step signal is inputted using a controller, and the eddy current retarder produces the resistance moment. The test data of the drawing force transducer are recorded and shown in Fig. 3.

As shown in Fig. 3, when inputting the step signal, $U(t) = 10$, at point $t = 8$ s, the transient response of the traction force is shown as the AB segment and the rectangular coordinates system is established by using point A as the origin. The changing relation $F(t)$ between traction force and

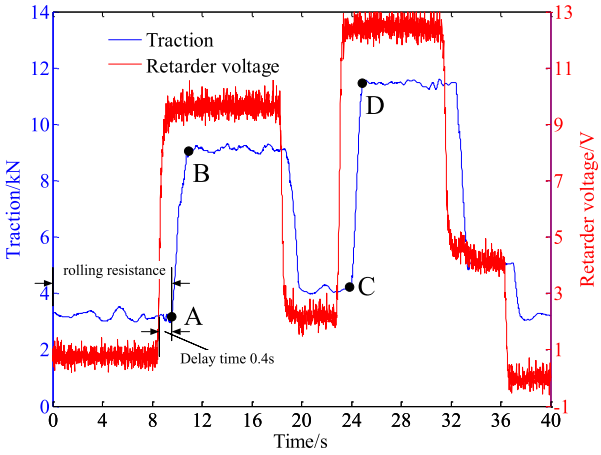

FIGURE 3. Result of the experiment.

time at the AB segment is obtained via fitting. The system transfer function, which regards retarder voltage as the input and traction as the output, is obtained by using the Laplace transform of the voltage signal function and the traction function, as shown in Equation (1):

$$G_1(s) = \frac{F_1(s)}{U_1(s)} = \frac{-0.014s^2 + 0.79s - 0.52}{s^2} \tag{1}$$

To test the validity and adaptability of the model, the step signal $U(t) = 10$ is applied at $t = 23$ s. The CD segment is the transient response of the traction to the step signal. The system transfer function is obtained using the same method described above.

The zero-point and pole-point distributions of the two system transfer functions are basically consistent; hence, the established system model is reliable. The system includes the delays caused by the current induced by the inductor and by the deformation of the elastic element, such as the traction device. The system transfer function also includes the delay time. The response time of the traction force to the retarder input voltage is 0.4 s. Therefore, the system transfer function, which regards the retarder voltage as the input and traction as the output, is

$$G(s) = \frac{-0.014s^2 + 0.79s - 0.52}{s^2} e^{-0.4s} \tag{2}$$

B. CONTROL ALGORITHM FOR RETARDER LOADING

On the basis of the random and time-varying nature of the retarder load, the BP neural network PID control algorithm is used to load the retarder; this control algorithm can adjust the PID control parameters in real time via online learning to obtain the best PID combination. The control structure is shown in Fig. 4.

In Fig. 4, $F_{in}(k)$ is the output load expectation for the retarder, $F_{out}(k)$ is the difference between the measured value of the output load of the loading system and the engine output load, $e(k)$ is the kth sample of the difference between $F_{in}(k)$ and $F_{out}(k)$, and $U(t)$ is the control voltage of the retarder.

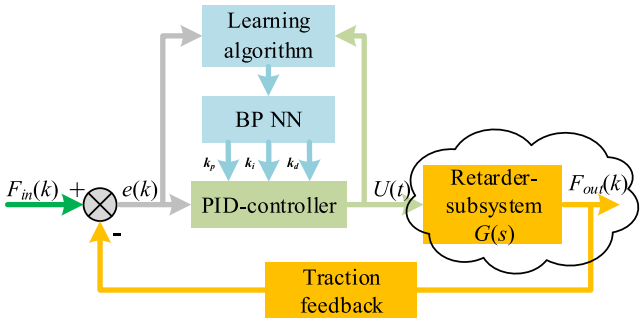

FIGURE 4. Structure of the BP-PID control system.

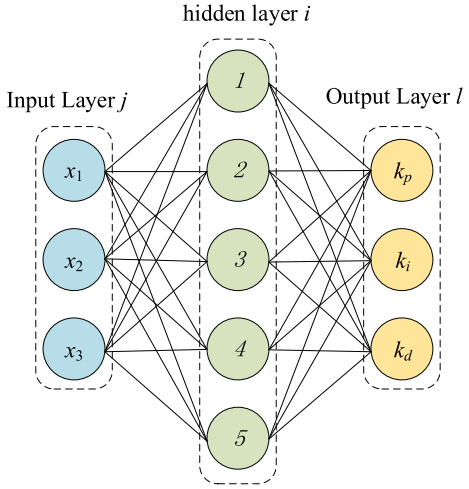

FIGURE 5. Structure of BP neural network.

Incremental PID control algorithm is

$$u(k) = u(k-1) + \Delta u(k) \tag{3}$$

$$\Delta u(k) = k_p(e(k) - e(k-1)) + k_i e(k) + k_d(e(k) - 2e(k-1) + e(k-2)) \tag{4}$$

The structure of BP neural network is shown in Fig. 5.

The neural network structure is 3*5*3, j is the input layer, i is the hidden layer, and l is the output layer.

The network input vector is

$$\begin{cases} x_1 = F_{in}(k) \\ x_2 = F_{out}(k) \\ x_3 = e(k) \end{cases} \tag{5}$$

The input layer neurons are

$$O_j^{(1)} = x_j \quad (j = 1, 2, 3) \tag{6}$$

Input and output of the hidden layer is

$$\begin{cases} net_i^{(2)}(k) = \sum_{j=1}^{4} \omega_{ij}^{(2)} O_j^{(1)}(k) - \theta_i^{(2)} \\ O_i^{(2)}(k) = f\left(net_i^{(2)}(k)\right) \quad (i = 1, 2, 3, 4, 5) \end{cases} \tag{7}$$

where ω is weight variation, θ is threshold.

Sigmoid functions as hidden layer nerve cells' activations function is

$$f(x) = \tan h(x) = \frac{e^x - e^{-x}}{e^x + e^{-x}} \tag{8}$$

Input and output of the output layer is:

$$\begin{cases} net_l^{(3)}(k) = \sum_{i=1}^{5} \omega_{li}^{(3)} O_i^{(2)}(k) - \theta_l^{(3)} \\ O_l^{(3)}(k) = g\left(net_l^{(3)}(k)\right) \\ O_1^{(3)}(k) = k_p \\ O_2^{(3)}(k) = k_i \\ O_3^{(3)}(k) = k_d \\ l = 1, 2, 3 \end{cases} \tag{9}$$

Output layer nerve cells' activations function is

$$g(x) = \frac{1}{2}(1 + \tan h(x)) = \frac{e^x}{e^x + e^x} \tag{10}$$

The target function of network performance is

$$E(k) = \frac{1}{2}[F_{in}(k) - F_{out}(k)]^2 = \frac{1}{2}e^2(k) \tag{11}$$

In BP neural network online learning, the relevance rating is adjusted based on the weighted coefficient of the negative gradient direction search, according to $E(k)$, and an inertial term is added to search for the quick convergence global minimal is

$$\Delta\omega_{li}^{(3)}(k) = -\eta\frac{\partial E(k)}{\partial\omega_{li}^{(3)}} + \alpha\Delta\omega_{li}^{(3)}(k-1) \tag{12}$$

where, $\Delta\omega_{li}^{(3)}(k)$ is the kth weight variation, η is learning rate, and α is the inertial coefficient.

$$\begin{cases} \frac{\partial E(k)}{\partial\omega_{li}^{(3)}} = \frac{\partial E(k)}{\partial y(k)}\frac{\partial y(k)}{\partial\Delta u(k)}\frac{\partial\Delta u(k)}{\partial O_l^{(3)}(k)}\frac{\partial O_l^{(3)}(k)}{\partial net_l^{(3)}(k)}\frac{\partial net_l^{(3)}(k)}{\partial\omega_{li}^{(3)}} \\ \frac{\partial net_l^{(3)}(k)}{\partial\omega_{li}^{(3)}} = O_i^{(2)}(k) - 2 \end{cases} \tag{13}$$

Symbolic function $sgn(\frac{\partial y(k)}{\partial\Delta u(k)})$ replace $\frac{\partial y(k)}{\partial\Delta u(k)}$

Formula (14) is calculated using formula (3), (4), (9)

$$\begin{cases} \frac{\partial\Delta u(k)}{\partial O_1^{(3)}(k)} = e(k) - e(k-1) \\ \frac{\partial\Delta u(k)}{\partial O_2^{(3)}(k)} = e(k) \\ \frac{\partial\Delta u(k)}{\partial O_3^{(3)}(k)} = e(k) - 2e(k-1) + e(k-2) \end{cases} \tag{14}$$

The learning algorithm of output layer weight variation is

$$\begin{cases} \Delta\omega_{li}^{(3)}k = \partial\Delta\omega_{li}^{(3)}(k-1) + \eta\delta_l^{(3)}O_i^{(2)}(k) \\ \delta_i^{(3)} = e(k)sgn(\frac{\partial y(k)}{\partial\Delta u(k)})\frac{\partial\Delta u(k)}{\partial O_l^{(3)}(k)}g'(net_l^{(3)}(k)) \end{cases} \tag{15}$$

The learning algorithm of hidden layer weight variation is

$$\begin{cases} \Delta\omega_{ij}^{(2)}(k) = \alpha\Delta\omega_{ij}^{(2)}(\text{k-1}) + \eta\delta_i^{(2)}O_j^{(1)}(k) \\ \delta_i^{(2)} = f'(net_i^{(2)}(k))\sum_{i=1}^{3}\delta_l^{(3)}\omega_{li}^{(3)}(k) \end{cases} \tag{16}$$

where

$$g'(\bullet) = g(x)(1-g(x)), \quad f'(\bullet) = (1-f^2(x))/2$$

C. CONTROL PERFORMANCE SIMULATION

The input of the retarder loading system should be a random load time domain model. Hence, the filter white noise generation method is used in the traction power spectral density function to reconstruct the traction time domain model.

The standard normal distribution white noise constructed using two independent [0, 1] uniformly distributed white noise sequences, η_1 and η_2, is

$$\zeta = (-2\ln\eta_1)^{1/2}\cos 2\pi\eta_2. \tag{17}$$

The normal distribution of white noise, which has the same mean value μ and variance σ^2 as the traction time domain model, is

$$X(t) = \mu + \sigma\zeta \tag{18}$$

The power spectrum of the response function of the normal distribution white noise is the same as the traction power spectrum when the filter is designed. The transfer function of the filter is $W(s)$, the impulse response function is $g(t)$, and the frequency response function is $H(f)$. The power spectral function of the input signal $X(t)$ is $G_N(f)$, and the output signal is the traction time domain signal $X_L(t)$, the power spectral function of which is $G(f)$. In accordance with linear system theory:

$$G(f) = |H(f)|^2 G_N(f) = 2\Delta t\,|H(f)|^2 D \tag{19}$$

where D is the load variance and Δt is the sample interval.

$$g(t) = L^{-1}[W(s)] \tag{20}$$

$$X_L(t) = g(t) * X(t) \tag{21}$$

Equation (9) is discretized as

$$out(k) = 0.5\Delta t\sum_{n=0}^{k}[g(k-n) + g(k-n+1)in(n)] \tag{22}$$

From the literature [20], [21], the traction standard unilateral power spectrum of the single-peak function of tractors in the field plowing conditions is

$$G^*(f) = \frac{G(f)}{D} = \frac{2\alpha(\alpha^2+\beta^2+f^2)}{\pi(\alpha^2-\beta^2+f^2)+4\alpha^2\beta^2} \tag{23}$$

where $G^*(f)$ is the standardized self-power spectral function, α and β are model parameters, and f is the frequency.

When Equation (19) is substituted into Equation (23), $|H(f)|^2$ is obtained. After determining the spectral resolution, the transfer function $W(s)$ of the filter is then obtained, and the impulse response function $g(t)$ of the filter is derived using Equation (21) through Laplacian inverse transform. When $g(t)$ is inputted into Equation (22), the traction time domain model is as shown in Fig. 8. In the black dot line waveform, the mean value is 11.49 kN and the variance is 4.99 $(\text{kN}\bullet\text{m})^2$.

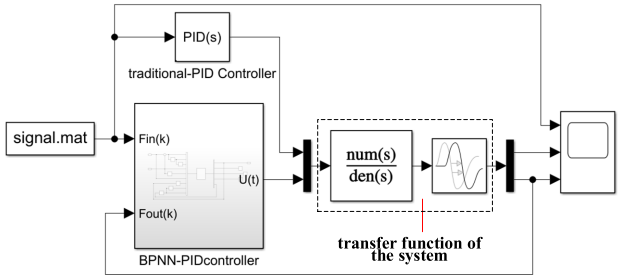

FIGURE 6. Simulink model of retarder loading system.

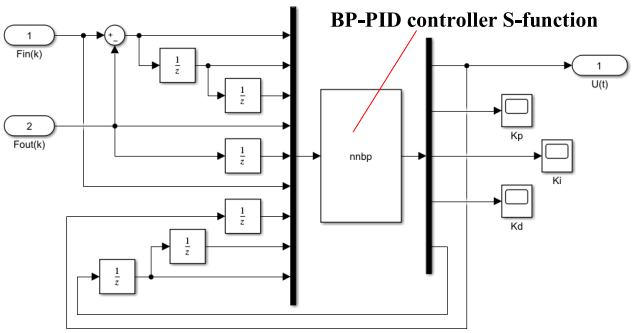

FIGURE 7. Structure of BPNN-PID controller.

MATLAB is used to accomplish discretization of the required transfer function, with a random signal as input and the traditional PID and BP-PID as the control algorithms. The simulation of the retarder loading performance is completed to check the response characteristics of the system and to verify the validity of the BP-PID control algorithm. The BP-PID control simulation model and the traditional PID control simulation model of the retarder loading system were established, as shown in Fig. 6. Fig. 7 shows the BPNN-PID controller model in Fig. 6.

A set of traction random signals is selected as system inputs, the engine output load is set as zero, and a set of improved parameters ($K_P = 5$, $K_I = 1.87$, $K_D = 0.3$) of the traditional PID control is selected to perform comparative analysis. $\eta = 0.25$, $\alpha = 0.05$. The simulation results are shown in Fig. 8.

As shown in Fig. 8, the load output of the load system with BP-PID control exhibits a better follow-up effect on the input than that with the traditional PID control. At the beginning of 0-5s, when the traction force suddenly increases from 0, the output traction force produces a large overshoot, and then gradually returns to stability. At $t = 14.1$s, the maximum difference between the output traction and the input traction, the difference is 398 N, and the error is 2.8%. The maximum delay of output traction is 56.5ms.

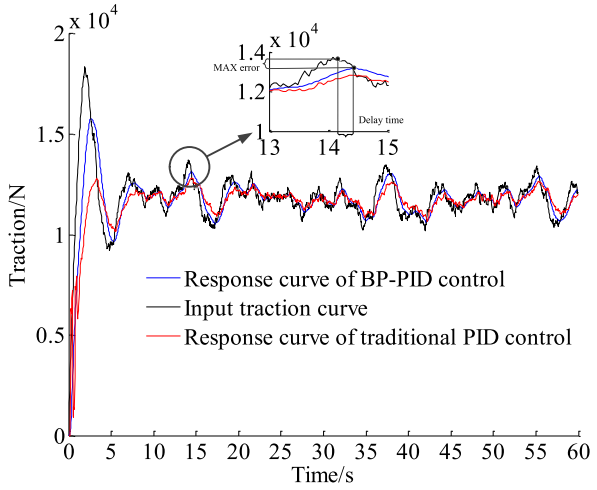

FIGURE 8. Response curve of retarder loading output.

FIGURE 9. Tractive characteristic test of the tractor.

V. DYNAMIC LOADING SYSTEM ROAD TEST

The traction test is performed with the YTO-MF554 tractor as the test vehicle to verify the performance of the system.

Test conditions: the test road is concrete with a slope of less than 0.5%, balancing weight is present, the height between the traction point and the ground is 580 mm, fuel temperature is 20.4°C, coolant temperature is 74.6°C, lubricant temperature is 79.2°C, front tire pressure is 100 kPa, rear tire pressure is 100 kPa, atmospheric temperature is 22°C, air pressure is 100 kPa, the relative humidity of the environment is 45%, the gear of the power wagon is in mid-II, the throttle lever position is 50%, and the tested gear of the test vehicle is in low III.

Test scheme: (1) The power wagon is dragged by the test vehicle, with the power wagon in mid-II gear and the test vehicle in neutral gear. The rolling resistance of the test vehicl is obtained using a tension sensor. (2) The electric eddy current retarder does not generate brake torque. The power wagon engine provides the driving force and follows the test vehicle until 30 m. The power radius of the driving wheel is calculated. (3) The gear of the power wagon is in mid-II and the throttle lever position is 50%. Then, the gear of the test vehicle is set to low-III and the throttle lever position is 100%. The power wagon is driven by the test vehicle with a speed of 7–8 km/h. The test site is shown in Fig. 9.

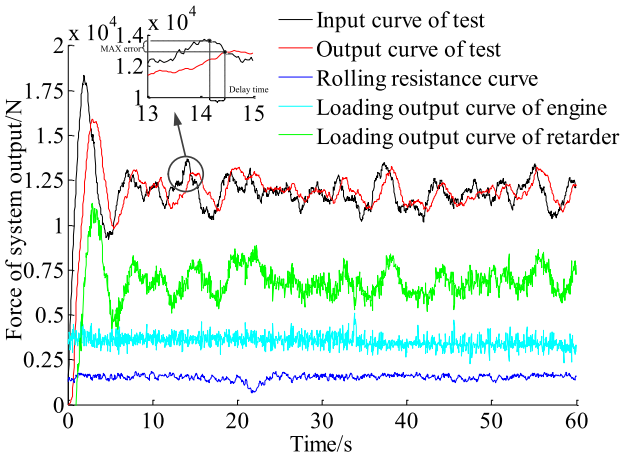

FIGURE 10. System output loading curves.

The response curve of the system test output load to the input load under the test gear is shown in Fig.10.

As shown in Fig. 10, rolling resistance is maintained at nearly 1.5 kN. Relatively large fluctuation occurs at $t = 22$ s due to the impact of the test road rolling resistance coefficient. The output load mean value of the test engine is 3.65 kN because the speed is 7–8 km/h. Speed changes within a small range, thereby causing fluctuations of the output load. The output load of the retarder is efficient at compensating for the remaining desired input load. The resulting effect of the output load is good for the input load, and the effect is better in accordance with the simulation load. The maximum delay of the system is 85.6 ms, and the maximum overshoot is 3.5%.

VI. CONCLUSION

1) This study analyzed and determined the relationship among power wagon engine resistance moment, gear, governor handle position, and speed. Engine load characteristics were also summarized.

2) A control strategy based on BP-PID was introduced for the retarder subsystem and its load performance was simulated. The simulation results showed that the maximum delay of the subsystem is 56.5 ms and the maximum output error is less than 2.8%. The multi-operating mode of a tractor in the field can be simulated by the power wagon on concrete. The results of the road tests showed that the maximum delay of the loading system is 85.6 ms and the maximum output error is less than 3.5%.

REFERENCES

[1] S. Zhang, Y. Du, Z. Zhu, E. Mao, J. Liu, and J. Shi, "Integrated control method of traction & slip ratio for rear-driving high-power tractors," *Trans. Chin. Soc. Agricult. Eng.*, vol. 32, no. 12, pp. 47–53, 2016.

[2] S. Kumar, M. T. Noori, and K. P. Pandey, "Performance characteristics of mode of ballast on energy efficiency indices of agricultural tyre in different terrain condition in controlled soil bin environment," *Energy*, vol. 182, pp. 48–56, Sep. 2019.

[3] K. D. R. Zhang Li Zheng and W. Yin, "Study of a Self-excited and Liqui d-cooled Electromagnetic Retarder," *Trans. Chin. Soc. Agricult. Machinery*, vol. 11, no. 4, pp. 20–26, 2014.

[4] H. Xu, R. He, and X. Wu, "Influence of retarder on brake stability of tractor-semitrailer," *China Mech. Eng.*, vol. 26, no. 17, pp. 2394–2399, 2015.
[5] X. Zhao, C. Ji, W. Zhou, G. Zhao, and Z. Lu, "Braking ability of vehicle united brake based on permanent magnet type eddy current retarder," *Trans. Chin. Soc. Agricult. Eng.*, vol. 25, no. 12, pp. 119–123, 2009.
[6] C. Xu and H. Yu, "A research on associated braking system for articulated vehicles with eddy retarder," *Automobile Eng.*, vol. 28, no. 4, pp. 366–369, 2006.
[7] S. Anwar, "A parametric model of an eddy current electric machine for automotive braking applications," *IEEE Trans. Control Syst. Technol.*, vol. 12, no. 3, pp. 422–427, May 2004.
[8] H. Ren, F. Yi, and J. He, "A computation method for braking torque of eddy current retarder," *Automot. Eng.*, vol. 26, no. 2, pp. 197–200, 2004.
[9] Y. Qu, D. Ning, Z. Lai, Q. Cheng, and L. Mu, "Neural networks based on PID control for greenhouse temperature," *Trans. Chin. Soc. Agricult. Eng.*, vol. 27, no. 2, pp. 307–311, 2011.
[10] Y. Chen, L. Chen, X. Xu, and C. Huang, "Vehicle height control of electronic-controlled air suspension under random disturbance," *Trans. Chin. Soc. Agricult. Machinery*, vol. 42, no. 12, pp. 309–315, 2015.
[11] L. Yang, B. Ma, and H. Li, "Steering neural network PID control for tracked vehicle with hydrostatic drive," *Trans. Chin. Soc. Agricult. Machinery*, vol. 41, no. 7, pp. 15–20, 2010.
[12] S. H. X. Wang Dou Sun and C. Yin, "Vehicle height adjustment and attitude control of electronically controlled air suspension," *Trans. Chin. Soc. Agricult. Machinery*, vol. 46, no. 10, pp. 335–342, 2015.
[13] J. Xie, K. Yan, and Y. Chen, "Synthesis of planar motion generation mechanisms using BP neural networks," *Chin. J. Mech. Eng.*, vol. 281, no. 2, pp. 24–27, 2005.
[14] Y.-H. Yang and Y. Shi, "Application of improved BP neural network in information fusion Kalman filter," *Circuits, Syst., Signal Process.*, vol. 39, no. 10, pp. 4890–4902, Oct. 2020.
[15] Y. He, Z. Meng, H. Xu, and Y. Zou, "A dynamic model of evaluating differential automatic method for solving plane problems based on BP neural network algorithm," *Phys. A, Stat. Mech. Appl.*, vol. 556, Oct. 2020, Art. no. 124845.
[16] F. Ding, X. Jia, T. Hong, and Y. Xu, "Flow stress prediction model of 6061 aluminum alloy sheet based on GA-BP and PSO-BP neural networks," *Rare Metal Mater. Eng.*, vol. 49, no. 6, pp. 1840–1853, Jun. 2020.
[17] L. Chen, F. Zhang, and L. Sun, "Research on the calibration of binocular camera based on BP neural network optimized by improved genetic simulated annealing algorithm," *IEEE Access*, vol. 8, pp. 103815–103832, 2020.
[18] X. Li, C. Yuan, and B. Shan, "System identification of neural signal transmission based on backpropagation neural network," *Math. Problems Eng.*, vol. 2020, pp. 1–8, Aug. 2020.
[19] L. Han, R. Li, and H. Zhu, "Comprehensive evaluation model of soil nutrient based on BP neural network," *Trans. Chin. Soc. Agricult. Machinery*, vol. 42, no. 7, pp. 109–115, 2011.
[20] Z. Fang, Z. Zhou, T. Yang, W. Zhang, J. Zhang, F. Liu, and X. Guan, "The power spectral function of the random loads in tractor," *J. Luoyang Inst. Technol.*, vol. 4, pp. 3–5, 1999.
[21] Z. Fang, Z. Zhou, T. Yang, W. Zhang, J. Zhang, F. Liu, and X. Guan, "Computer simulation for normal random load," *J. Luoyang Inst. Technol.*, vol. 1, pp. 1–3, 2000.

XIANGHAI YAN is a University Lecturer. He has rich practical experience in the field of vehicle testing. His main research interests include vehicle test method and technology, power matching of the transmission system of agricultural vehicles and road transport vehicles, and design and testing of steering control. He is a member of the Chinese Mechanical Engineering Society.

QIANWEN TAO was born in Zhengzhou, Henan. She received the bachelor's degree from the Henan University of Science and Technology, in 2015, where she is currently pursuing the degree. Her current research interest includes electric agricultural machinery experimental technology research.

LIYOU XU is a Professor. He is also a Ph.D. Supervisor. His research interests include new vehicle transmission theory and control technology, vehicle performance analysis method and simulation technology, and low-speed electric vehicle transmission technology. He is a Council Member of the Chinese Society of Automotive Engineering. He is a member of the Tractor Branch of Chinese Society of Agricultural Machinery, and the Youth Working Committee of Chinese Society of Agricultural Machinery.